JOURNAL OF GEOPHYSICAL RESEARCH, VOL. 99, NO. A3, PAGES 4095–4104, MARCH 1, 1994

Effect of the relative flow velocity on the structure and stability of the magnetopause current layer

M. M. Kuznetsova

Space Research Institute, Russian Academy of Sciences, Moscow

M. Roth

Institut d'Aéronomie Spatiale de Belgique, Brussels

Z. Wang and M. Ashour-Abdalla

Department of Physics and Institute of Geophysics and Planetary Physics, University of California, Los Angeles

The Vlasov kinetic approach is used to study the stability of the magnetopause current layer (MCL) when a sheared flow velocity and a sheared magnetic field both exist simultaneously within it. A modified Harris–Sestero equilibrium where the magnetic field and bulk velocity are changing direction on the same spatial scale is suggested to illustrate the generation of a y component of the magnetic field in the center of the MCL. With this equilibrium it is shown that $B_y(0)$ can be of the order of $B_z(\infty)$ when the value of the shear flow (U) tends to the ion drift velocity (U_d). The modifications of the initial symmetrical Harris configuration, introduced by the presence of a shear flow, strongly influence the adiabatic interaction of the plasma with low-frequency tearing-type electromagnetic perturbations as well as the nonadiabatic response of the particles near the center of the MCL. This results in a reduction of the growth rate of the tearing mode.

1. Introduction

Studies of the structure of the magnetopause current layer (MCL) and of its stability with respect to the excitation of large-scale perturbations (for example, tearing mode or Kelvin-Helmholtz instability) play an important role in understanding mass and energy transfer from the solar wind to the magnetosphere. The conditions of spontaneous excitation of longwave perturbations (wavelength $\Lambda_k = 2\pi/k$ much greater than the thickness of the layer L) depend not only on the local values of the plasma parameters near a given magnetic surface within the MCL but mainly on the global distribution of magnetic and electric fields, particle number densities, and tangential flow velocity profiles across the MCL, that is, on the initial equilibrium structure of the layer which determines the free energy of the perturbations. This circumstance significantly complicates the theoretical study of the global stability of the MCL. These difficulties are reflected on two theoretical approaches generally considered in the abundant literature devoted to this subject.

The first approach, and the most fundamental one, is based on the kinetic Vlasov formalism (see, for example, *Drake and Lee* [1977], *Galeev and Zelenyi* [1977], *Coppi et al.* [1979], *Quest and Coroniti* [1981], *Kuznetsova and Zelenyi* [1985, 1990a], *Galeev et al.* [1986], and references therein). In these papers the initial equilibrium structure is the well-known Harris configuration [*Harris*, 1962] generalized for the case where the plasma is magnetized by the constant current-aligned magnetic field component B_y

$$\mathbf{B} = B_0 \tanh(x/L)\mathbf{e_z} + B_y\mathbf{e_y}, \quad B_y = \text{const} \qquad (1)$$

This model describes the main property of the MCL, the rotation of the magnetic field vector across the layer. *Galeev et al.* [1986] have obtained the general stability thresholds for the destruction of all magnetic surfaces within the configuration (1) due to the excitation of drift tearing instabilities. In this study the marginal thickness L of the MCL is computed as a function of θ_0, the total angle of rotation of the magnetic field. The approach by *Galeev et al.* [1986] is, however, not appropriate for the case of nearly opposite directions of magnetosheath and magnetospheric magnetic fields (in the angular interval: $120° < \theta_0 < 180°$, $B_y \ll B_0$) when configuration (1) tends to the one-dimensional "neutral sheet" limit. Indeed, in this case the drift theory breaks down, and the stability analysis based on model (1) gives very reduced values of the critical magnetopause thickness ($L \leq \rho_i$, where ρ_i is the Larmor radius of the magnetosheath ions). Although many magnetopause crossings are characterized by a magnetic field rotation close to 180° [e.g., *Berchem and Russell*, 1982*b*], one-dimensional neutral sheets ($B_y \to 0$) as well as layers with a constant or nearly constant value of B_y are seldom observed. What is actually observed is a systematic variation of both B_y and B_z as the satellite passes through the magnetopause, while the quantity $B_y^2 + B_z^2$ remains approximately constant even for $\theta_0 \to 180°$.

Another disadvantage of the model (1) is that it describes an absolutely symmetrical MCL composed of a population

Paper number 93JA02358.
0148-0227/94/93JA-02358$05.00

of "trapped" particles "isolated" from the magnetosheath and magnetosphere plasmas. The latter can only be introduced in the model in the form of a uniform background [*Kuznetsova and Zelenyi*, 1990*b*]. Observations show, however, that the magnetopause is a mixture of plasmas of both magnetosheath and magnetospheric origins [*Bryant and Riggs*, 1989]. To understand how the magnetosheath parameters control the stability of the MCL, factors of asymmetry should be introduced in the equilibrium model, which can be considered as a tangential discontinuity (TD). These factors of asymmetry should emphasize the difference between magnetosheath parameters just outside the magnetopause (tangential flow velocity, number density, absolute value of magnetic field, and temperature) and those in the magnetosphere. They should finally appear as parameters in the formulation of the stability thresholds.

Some kinetic studies of the Kelvin-Helmholtz (K-H) instability in layers with flow velocity asymmetry but without magnetic shear (magnetic field in the same direction on both sides of the layer) have also been performed [*Ganguli et al.*, 1988; *Pu*, 1989; *Cai et al.*, 1990; *Wang et al.*, 1992]. These results can be applied for the case of northward orientation of the interplanetary magnetic field away from the stagnation point. However, when the interplanetary magnetic field has a southward orientation, a sheared velocity and a sheared magnetic field both exist simultaneously within the MCL.

Particle simulation of the formation and evolution of the MCL has been carried out by *Berchem and Okuda* [1990, and references therein]. *Cargill and Eastman* [1991] presented results of hybrid simulations where electrons were treated as a massless fluid, and the ions were treated as particles. A considerable amount of effort has been made after the pioneering work of *Sestero* [1966] to construct a self-consistent equilibrium Vlasov model of realistic TDs with large magnetic shear ($\theta_0 > 90°$) and asymmetrical boundary conditions (see, for example, *Kan* [1972], *Lemaire and Burlaga* [1976], *Roth* [1978, 1979, 1984], *Lee and Kan* [1979], and references therein). However, none of these models were used for stability analysis of the MCL using the Vlasov formalism.

The second approach used in the study of the global stability of the MCL is based on MHD simulations of the coupling between the tearing mode and the K-H instability [*Liu and Hu*, 1988; *La Belle-Hamer et al.*, 1988; *Hu et al.*, 1988; *Pu and Yei*, 1990; *Pu et al.*, 1990*a*, *b*]. The influence of shear flow on the double tearing instability in the frame of incompressible viscoresistive MHD was also considered by *Ofman* [1992, and references therein]. For the former case the initial configuration is characterized by a one-dimensional Harris profile of the magnetic field which reverses direction together with a similar antisymmetrical profile of the parallel bulk flow

$$\mathbf{B}(x) = B_0 \tanh(x/L)\mathbf{e_z}, \quad \mathbf{V}(x) = -V_0 \tanh(x/L)\mathbf{e_z} \quad (2)$$

The problem of determining the velocity distribution functions corresponding to configuration (2) is not discussed within the framework of the MHD approach. It is assumed that the effect of the velocity shear on the structure of the equilibrium magnetic field can be neglected when the relative flow velocity is much smaller than the thermal velocity of the plasma. Within the framework of this assumption it is shown that the growth rate of the tearing mode is only slightly modified by the shear flow up to the Mach number $M_a = 1$. It was also argued by *Pu and Yei* [1990] that the addition of a B_y magnetic field component does not influence the stability properties of the MCL, as the coupling of that component with V_z and B_z was thought to be absent. We will, however, show in sections 3 and 5 that the presence of a shear flow will modify the profile of $B_y(x)$ and, consequently, the growth rate of the tearing mode.

To study the influence of the shear flow on the tearing mode, attempts have also been made to combine the MHD and kinetic approaches by separating the plasma into two regions: an internal "kinetic region," where the Vlasov formalism is used, and an external "MHD region" where the system of MHD equations is solved [*Lakhina and Schindler*, 1983*a*, *b*; *Zelenyi and Kuznetsova*, 1984; *Wang and Ashour-Abdalla*, 1992].

The coupling between K-H and tearing modes was investigated by *Zelenyi and Kuznetsova* [1984] for the magnetotail configuration. In that work it was assumed that, inside the tail ($|x| < x^*$, where x^* is the half-thickness of the magnetotail), the plasma configuration can be described by the plain Harris model without flow (configuration (1) with $B_y = 0$). For the external solar wind flow ($|x| > x^*$) the incompressible MHD approximation was used. For this hybrid model the error in the definition of the plasma distribution functions (in comparison with self-consistent ones) is found proportional to $\exp(-2x^*/L)$, where L is the half-thickness of the plasma sheet. For the magnetotail configuration $x^* \gg L$, and, consequently, this error is very small.

For the dayside magnetopause, configuration (2) has been used by *Wang and Ashour-Abdalla* [1992] as the initial unperturbed equilibrium. The "boundary" between the external MHD region and the internal kinetic region is taken inside the plasma sheet. Therefore the error in the definition of the equilibrium configuration could be rather large. In other words, the plasma and field distributions in the external region (for example, the asymmetry in the flow velocity on both sides of the layer) may change the plasma and field distributions in the inner region and vice versa. It is realistic to think that the plasma and field distributions inside the layer could be significantly modified when the relative flow velocity exceeds the drift velocity corresponding to the diamagnetic current which supports the magnetic field reversal. It is clear that the uncertainties in determining the initial equilibrium configuration will result in nonrealistic estimates from the stability analysis (stability thresholds and growth rates).

In this work we are investigating, using Vlasov formalism, the influence of the flow asymmetry on the structure and stability of the MCL for the case of nearly oppositely directed asymptotic magnetic fields, that is, for large rotation angles of the magnetic field ($120° \ll \theta_0 \leq 180°$).

In section 2 we discuss some problems that can arise in the kinetic formulation of the configuration (2) generally used in MHD simulations.

To illustrate the modifications of the Harris neutral sheet (configuration (1) with $B_y \ll B_0$) by the flow asymmetry we present, in section 3, an equilibrium model which is a combination of the models of *Harris* [1962] and *Sestero* [1966]. To illustrate this new model, we display the numerical profiles of the unperturbed magnetic field, electric potential, number density, and bulk flow velocity for different values of u, the flow asymmetry factor ($u = |V_1 - V_2|/2U_d$, where

V_1 is the bulk flow velocity in the magnetosheath, V_2 is the bulk velocity in the magnetosphere, and U_d is the ion drift velocity). This model is reduced to the Harris plane neutral sheet when the factor u tends to zero.

In sections 4 and 5 we carry out the kinetic stability analysis of this simplest self-consistent asymmetrical equilibrium model. In section 4 we obtain a generalized eigenmode equation for the tearing mode, using the differential approximation for the perturbed vector potential and integrating along the particle trajectory. In section 5 we make analytical estimates to show some of the basic signatures of the tearing mode modified by the flow asymmetry and present a numerical solution of the generalized eigenmode equation. The paper ends in section 6 with a summary and the conclusions.

2. Kinetic Modeling of Magnetic Field Reversal in the Presence of Shear Flow

Let us consider a one-dimensional plane TD which is parallel to the y-z plane and which is not necessarily charge neutral. All plasma and field variables are then assumed to depend only on the x coordinate, normal to the layer. Because a TD has no normal component of the magnetic field, the latter lies entirely in the y-z plane, while the electric field $\mathbf{E}$ is parallel to the x axis. In this well-known configuration a single plasma particle of the j species ($j = e$ for the electrons, $j = i$ for the ions) is characterized by three constants of motion: the Hamiltonian (H_j)

$$H_j = m_j v^2/2 + e_j \phi \qquad (3)$$

and the y and z components of the canonical momentum (P_{jy} and P_{jz})

$$P_{jy} = m_j v_y + e_j a_y/c, \quad P_{jz} = m_j v_z + e_j a_z/c \qquad (4)$$

In these equations, c is the velocity of light in vacuum, e_j is the charge of the particle of mass m_j and $\mathbf{v}$ is (v_x, v_y, v_z) its velocity vector, while $\phi(x)$ is the electric potential, and (a_y, a_z) are the y and z components of the vector potential.

The simplest (and the most generally used) way to solve the Vlasov equation is to use single-valued velocity distribution functions in the (H, P_y, P_z) space. Macroscopic plasma parameters like the partial number densities n_j, the components of current densities J_{jy}, J_{jz}, or the bulk flow velocity V can then be obtained from the velocity distribution functions f_{0j} as functions of a_y, a_z, and ϕ.

If we are now considering a charge neutral plane current layer ($B_y = 0$, a_z and ϕ are constant values), then for single-valued f_{0j} the x dependence of plasma parameters can only be introduced through the $a_y(x)$ component of the vector potential. If we assume that the magnetic field $\mathbf{B} = B_z \mathbf{e_Z}$ reverses direction across the sheet

$$B_z(x) \rightarrow -B_0, \quad x \rightarrow -\infty \qquad (5a)$$

$$B_z(x) \rightarrow +B_0, \quad x \rightarrow +\infty \qquad (5b)$$

then the asymptotes of the function $a_y(x)$ on both sides of the MCL are symmetrical

$$a_y(x) \approx B(x)x \rightarrow |x|B_0, \quad x \rightarrow \pm\infty \qquad (6)$$

and, consequently, all plasma parameters (including the flow velocity $V_z(x)$) which depend on x only through $a_y(x)$ have equal values on both sides of the layer. For instance,

$$V_1 = V_z(x \rightarrow -\infty) = V_z(x \rightarrow +\infty) = V_2 \qquad (7)$$

For the odd Harris profile of the z component of the magnetic field [$B_z(x) = da_y(x)/dx$] the x dependence of all plasma parameters, expressed through the even function $a_y(x)$, should be even. In other words, the "cutoff" factor (see, for example, *Lee and Kan* [1979]) required in the distribution functions to separate the magnetosheath and magnetospheric particles (with different plasma parameters) cannot be introduced in the form of a single-valued dependence on P_y for the case of magnetic field reversal. This was also demonstrated in the paper by *Sestero* [1964] (see the discussion by *Sestero* [1964] of Figure 3). Note that for a one-dimensional magnetic field reversal, any deviation from charge neutrality ($\phi(x) \neq$constant) cannot help to "separate" both the ion and electron components of two plasmas with distinct characteristics. Indeed, the electric potential "acts" differently on both components. This results from the fact that all moments of the electron velocity distribution function are proportional to $\exp[+e\phi(x)/T_e]$, while those of the ion velocity distribution function are proportional to $\exp[-e\phi(x)/T_i]$ (here e is the magnitude of the electron charge, and T_e and T_i are the electron and ion thermal energies).

A way to introduce flow asymmetry in one-dimensional magnetic field reversal is to consider multivalued distribution functions in the (H, P_y) plane [*Sestero*, 1964; *Whipple et al.*, 1984]. This means that particle trajectories corresponding to the same values of H and P_y can be physically disconnected, and an additional parameter characterising the spatial region from which particles are unable to escape can be introduced. For our case, particles moving outside the neutral region ($|x| < (\rho_i L)^{1/2}$) will never cross the plane $x = 0$ and can be characterized by an additional invariant: sign(x). Inside the neutral region the flow velocity profile should be symmetrical. For thick MHD layers the extent of the symmetrical neutral region is negligible. On the contrary, for thin kinetic layers typical of the magnetopause ($L < 10\rho_i$) [*Berchem and Russell*, 1982*a*] the extent of the symmetrical neutral region is at least $L/3$; and the flow configuration cannot be similar to that given by equation (2). For these kinetic layers the flow velocity is nearly constant in the central part, while the shear can only occur in the outer regions. This kind of flow velocity profile was modeled by *Lakhina and Schindler* [1983*a*, *b*] only for $x \geq 0$, using equilibrium distribution functions similar to those introduced by *Alpers* [1969].

In the next section we will consider another way for modeling an asymmetrical flow velocity profile by introducing a nonvanishing B_y component which does not reverse sign. Indeed, in most magnetopause crossings, observations show that the magnetosheath and magnetospheric magnetic fields are not strictly antiparallel and that the angle of rotation of the B vector is less than 180° [*Berchem and Russell*, 1982*b*].

3. Modification of the Harris Plane Configuration by a Flow Asymmetry

Across the TD considered in this section, the magnetic field $\mathbf{B}$ is assumed to rotate in the (y-z) plane (the total angle of rotation being θ_0; $\theta_0 < 180°$) and to have equal magnitudes $B_1 = B_2 = B(x \rightarrow \mp\infty)$ on magnetosheath ($x \rightarrow -\infty$) and magnetospheric ($x \rightarrow +\infty$) sides. In this case it is possible to choose the coordinate system in such a way that the B_z component is changing sign in the center of the MCL ($x = 0$) and has opposite asymptotic values: $B_z(x \to +\infty) = -B_z(x \to -\infty) = B_0$, while assuming B_y everywhere positive.

Let us introduce unperturbed velocity distribution functions which are combinations of distributions of *Harris* [1962] and *Sestero* [1966]. Sestero's contribution for a j plasma species will, however, be modified to take into account a thickness larger than the characteristic Larmor radius ρ_j of particles with thermal energy (temperatures) T_j in the asymptotic magnetic field B_1

$$\rho_j = \frac{c\sqrt{2m_jT_j}}{eB_1}, \quad j = e, i \tag{8}$$

Therefore the (P_y, P_z) dependence in Sestero's part will now be expressed in terms of complementary error functions, whose "half-thickness" is at least the Larmor radius, rather than in terms of step functions which always lead to maximum characteristic thicknesses equal to ρ_i (for observations of the magnetopause thickness, see *Berchem and Russell* [1982*a*]).

It can be seen that the following velocity distribution functions are quite appropriate

$$\begin{aligned} f_{0j} \;=\; & \frac{1}{2}\left(\frac{m_j}{2\pi T_j}\right)^{3/2} \exp\left(-\frac{2H_j + m_jU^2}{2T_j}\right) \\ & \cdot\left\{s_1 + s_0 \exp\left[-(\frac{\rho_j}{2D})^2 - \delta_{jy}P_{jy}\right]\right\} \\ & \cdot\left\{\text{erfc}\left[-\delta_{jz}(P_{jz} - m_jU)\right]\exp\left(\frac{UP_{jz}}{T_j}\right)\right. \\ & \left. + \alpha_j \text{erfc}\left[\delta_{jz}(P_{jz} + m_jU)\right[\exp\left(-\frac{UP_{jz}}{T_j}\right)\right\} \end{aligned} \tag{9}$$

where

$$\delta_{jz} = \frac{c}{e_jB_1\sqrt{D^2 - \rho_j^2}}, \quad \delta_{jy} = \frac{c}{e_jB_1D}, \quad \alpha_j = 1 \tag{10}$$

and erfc(u) is the complementary error function

$$\text{erfc}(u) = \frac{2}{\sqrt{\pi}} \int_u^{+\infty} \exp(-x^2)\, dx$$

The parameter D characterizes the thickness of the MCL. When D shrinks to ρ_j, the complementary error functions in (9) tend to the step functions introduced by *Sestero* [1966]. When U tends to 0, the distribution functions (9) tend to Maxwellian functions shifted by the diamagnetic drift velocity $U_{dj} = cT_j/e_jB_1D$, which for boundary conditions (5) correspond to Harris configuration (1). The parameter D is related to the L parameter of configuration (1) by the relation

$$L \approx 2DB_1/B_0 \tag{11}$$

The parameters s_0 and s_1 characterize, respectively, the distribution of "trapped" and "untrapped" particles. They are linked to the number density in the center of the layer (for s_0) and to the asymptotic number densities (for s_1) in a way that will be clarified when expressions for number densities will have been calculated.

Assuming the B_y component everywhere positive, it is easy to verify that the distributions (9) describe a MCL where a two-components plasma (electrons, ions) with symmetrical temperatures T_j is flowing at a velocity $(0, 0, U)$ on the magnetosheath side and at a velocity $(0, 0, -U)$ on the magnetospheric side (i.e., the profile of the bulk flow velocity is antisymmetrical).

If one assumes that $\alpha_i \neq 1$, then the distributions (9) describe a TD with asymmetrical profiles of the number density and corresponding magnetic field intensity. In this study we will, however, neglect these possible asymmetries in order to single out the effect of the relative flow velocity.

Note that the velocity distribution functions of the trapped particles in equation (9) differ from those introduced by *Lee and Kan* [1979, Equation 8]. The distribution of the trapped particles defined in equation (9) has been found more appropriate for configurations with large angles of magnetic field rotation and nonzero relative flow velocity.

From the velocity distribution functions given in (9) the number and current densities can be calculated as a function of (ϕ, a_y, a_z). It is found

$$n_j = \sum_{\nu=1}^{2} n_j^{(\nu)} \tag{12}$$

$$\begin{aligned} n_j^{(\nu)} = & \frac{1}{2}\left[s_1 + s_0 \exp(-\overline{a}_y)\right] \times \\ & \exp\left\{-\frac{q_j}{t_j}\left[\overline{\phi} + (-1)^\nu u\overline{a}_z\right]\right\} \text{erfc}\left[(-1)^\nu \overline{a}_z\right] \end{aligned} \tag{13}$$

$$J_{jz} = cT_j\frac{\partial n_j}{\partial a_z} \tag{14}$$

$$J_{jy} = cT_j\frac{\partial n_j}{\partial a_y} \tag{15}$$

where

$$t_j = \frac{T_j}{T_i}, \quad q_j = \frac{e_j}{e}, \quad \overline{a}_z = \frac{a_z}{B_1D}, \quad \overline{a}_y = \frac{a_y}{B_1D}, \quad \overline{\phi} = \frac{e\phi}{T_i}$$

and u is the factor of flow asymmetry

$$u = U/U_d, \quad U_d = cT_i/eB_1D \tag{16}$$

Assuming that $a_y(0) = a_z(0) = 0$, it is clear from the quasi-neutrality condition that $\phi(0) = 0$ and

$$\phi(x \to \mp\infty) = (U/c)B_y(x \to \mp\infty)|x| \tag{17}$$

From equations (12), (13), and (17) it can be seen that the parameter s_1 is equal to the symmetrical asymptotic number densities $[n_j(x \to \mp\infty) = s_1;\ j = e, i]$, while s_0 characterizes the number density in the center of the layer $[n_j(x = 0) = s_0 + s_1;\ j = e, i]$.

The structure of the MCL is given by the solutions of a set of two second-order differential equations for $a_y(x)$ and $a_z(x)$

$$\frac{d^2a_y}{dx^2} = -\frac{4\pi}{c}\sum_j J_{jy}(a_y, a_z, \phi) \tag{18}$$

$$\frac{d^2a_z}{dx^2} = -\frac{4\pi}{c}\sum_j J_{jz}(a_y, a_z, \phi) \tag{19}$$

coupled with the quasi-neutrality equation

$$n_e(a_y, a_z, \phi) = n_i(a_y, a_z, \phi) = n(x) \tag{20}$$

The differential equations (18) and (19) form a system of four differential equations of the first order for a_y, a_z, B_y, and B_z. This system is solved numerically using a Hamming's predictor-corrector scheme [*Ralston and Wilf*, 1965]. It is coupled with equation (20) whose solution is obtained by the Newton-Raphson method for finding the root of a nonlinear algebraic equation [*Press et al.*, 1986]. Starting from the central surface $x = 0$, the system is integrated toward the magnetosheath ($x \to -\infty$) up to the turning point x^*, where both components of the current density become negligibly small, and then back to the magnetosphere ($x \to +\infty$). For the starting values we choose

$$a_y(0) = a_z(0) = \phi(0) = 0,$$

$$a_y'(0) = B_z(0) = 0, \quad a_z'(0) = -B_y(0) \qquad (21)$$

The value of $B_y(0)$ can be obtained from the pressure balance condition

$$B_1^2 = 8\pi s_0(T_e + T_i) + B_y^2(0) \qquad (22)$$

We will now illustrate how the MCL structure is changing when the factor of flow asymmetry u is increased, while keeping the angle $\theta_0 \approx 170°$. In what follows, the MCL layer is characterized by the following plasma and field parameters: $B_1 = B_2 = 60$ nT, $T_i = T_e = 1$ keV, $\rho_i = 76.2$ km. The asymptotic number density s_1 on the magnetosheath and magnetospheric sides is chosen very small in comparison with the density inside the MCL (in order to compare with the Harris model), that is, $s_1 = 0.01$ cm$^{-3} \ll s_0$. On the other hand, the value of the input parameter s_0 is determined by the asymmetry factor u in the following way: for a fixed value of u, an iterative method is used to find the value of s_0 corresponding to $\theta_0 \approx 170°$, that is, to nearly opposite directions of the asymptotic magnetic fields. Table 1 gives some computed values of s_0 corresponding to a set of values of u, for $D = 1.5\rho_i$. Note that these values as well as profiles illustrated in Figures 1-3 practically do not depend on the ratio D/ρ_i.

Figures 1 and 2 illustrate the structure of the magnetopause for $u = 0.9$ and $u = 2$, respectively. Plasma and field parameters are illustrated as functions of the distance x/ρ_i from the center of the layer. The dashed curves in Figures 1 and 2 correspond to Harris profiles, that is, to the case where $u = 0$. The following variables are illustrated: B_z (in nanoteslas) (Figures 1*a* and 2*a*); bulk flow velocity V/V_{Ti} ($V_{Ti} = (2T_i/m_i)^{1/2}$ is the ion thermal velocity, $V_{Ti} = 438$ km/s) (Figures 1*b* and 2*b*); hodogram of the magnetic field (in nanoteslas) (Figures 1*c* and 2*c*); number density n (per cubic centimeters) (Figures 1*d* and 2*d*); $J_z^* = J_{iz}^* + J_{ez}^*$ is the z component of the total current density normalized to $\Lambda_J = s_1 e V_{Ti}$ ($= 7\times10^{-10}$ A/m^2) (Figures 1*e* and 2*e*); electric potential ϕ^*, normalized to $\Lambda_\phi = 2T_i/e$ ($= 2 \times 10^3$ V) (Figures 1*f* and 2*f*). It is seen from Figures 1*e* and 2*e* that the relative flow velocity results in a finite J_z component of the current density inside the MCL which generates the B_y component in the center of the layer.

Figure 1 shows that the Harris profiles of $B_z(x)$ and $n(x)$, corresponding to $u = 0$, are only slightly modified when u

TABLE 1. Computed Values of $s_0(u)$

u	s_0, cm^{-3}
2.	2.
1.615	3.
1.4	3.5
1.2	4.
0.9	4.2
0.	4.4

$u = U/U_d$, where U is the shear flow and U_d is ion drift velocity; s_0 is the parameter defined in equation (9) (for very small values of the number density on the magnetosheath and magnetospheric sides s_0 is nearly equal to the number density at the center of the MCL); and the total angle of rotation $\theta_0 \approx 170°$.

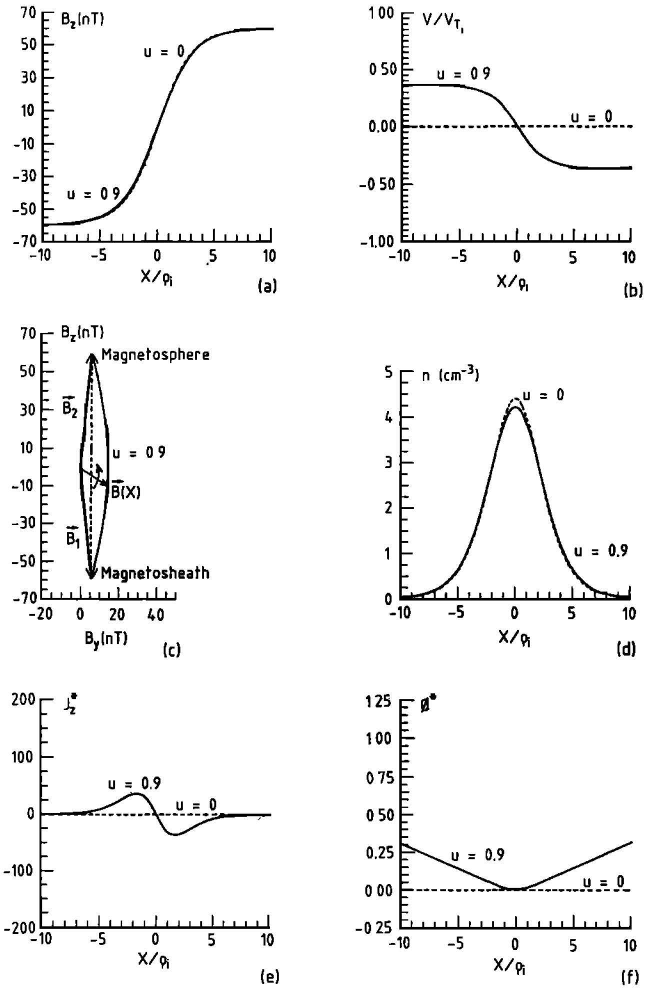

Fig. 1. Structure of the magnetopause current layer for $|B_1| = |B_2| = 60$ nT, $T_i = T_e = 1$ keV, $\theta_0 \approx 170°$, $u = 0.9$. The ratio $u = U/U_d$ is the factor of flow asymmetry. It represents half the relative flow ($U = |V_1 - V_2|/2$) normalized to the ion drift velocity $U_d = cT_i/eB_1D$ (=146 km/s for the plasma and field parameters used here). The total angle of rotation of the magnetic field is θ_0. For comparison, the Harris profiles corresponding to $u = 0$ are also displayed and are represented by the dashed curves. From left to right and from top to bottom the following variables are illustrated. (a) B_z (in nanoteslas); (b) bulk flow velocity V/V_{Ti} ($V_{Ti} = (2T_i/m_i)^{1/2}$ is the ion thermal velocity; $V_{Ti} = 438$ km/s); (c) hodogram of the magnetic field (in nanoteslas); (d) number density n (per cubic centimeters); (e) $J_z^* = J_{iz}^* + J_{ez}^*$ is the z component of the total current density normalized to $\Lambda_J = s_1 e V_{Ti}$ (=7×10^{-10} A/m^2); (f) electric potential ϕ^*, normalized to $\Lambda_\phi = 2T_i/e$ (=2×10^{3}V). These plasma and field parameters are illustrated as a function of the distance x/ρ_i from the center of the layer (where ρ_i is the ion Larmor radius in the field B_1; $\rho_i = 76.2$ km). The configuration is also characterized by the following parameters: $D = 1.5\rho_i \approx 114$ km, $s_1 = 0.01$ cm^{-3}. The value of the parameter s_0 depends on the value of u as determined in Table 1.

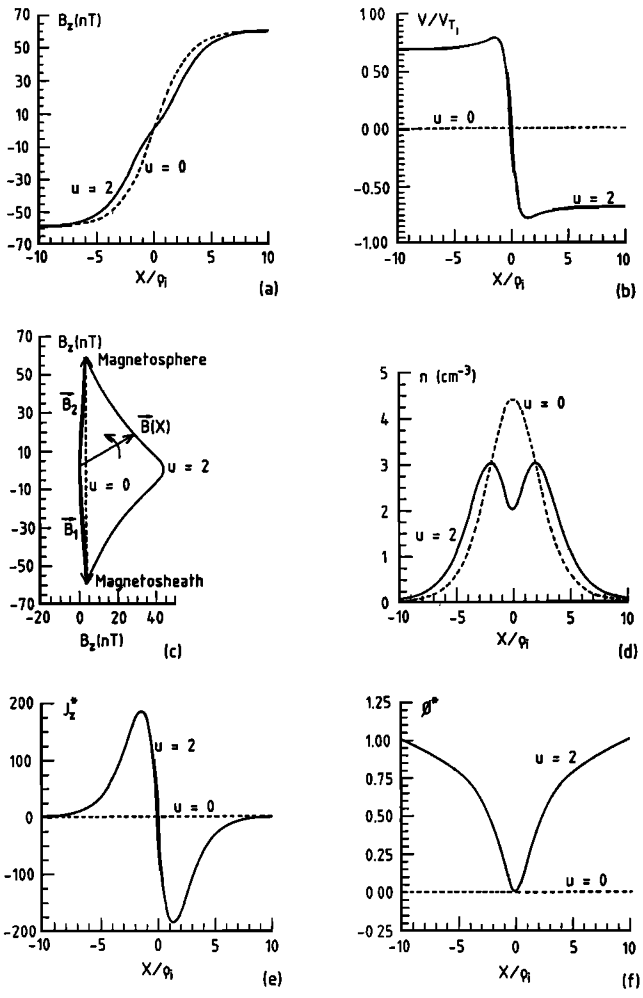

Fig. 2. Same as figure 1, but for the case $u = 2$.

has a nonzero value less than 1 (i.e., $U \leq U_d$). Figure 2 shows that when $u = 2$, the $B_z(x)$ and $n(x)$ profiles differ more strongly from the Harris case. Note that the density has now 2 maxima, separated by a minimum at the center of the layer. This is due to the increase of the magnetic pressure near $x = 0$. Indeed, the hodogram shows that when $|x| \rightarrow 0$, the B_y increase is larger than the B_z decrease. It can also be seen that the J_z component and associated B_y component increase with u.

Profiles of the B_y component of the magnetic field for different values of u are shown on Figure 3. It is seen that B_y can reach significant values when $u \approx 1 \div 2$, that is, when the relative flow velocity U is of the order of the ion drift velocity (U_d), which is much less than the ion thermal velocity [$U_d = V_{Ti}\ (\rho_i/2D) \ll V_{Ti}$], especially for thick layers $2D/ \gg \rho_i$ (see also Figure 4). We see that in the presence of a relative flow (along the component of the magnetic field which reverses sign) there is no neutral plane. Even for practically opposite direction of magnetic fields on both sides of the layer, the absolute value of the magnetic field does not equal 0 in the center of the layer where $x = 0$.

The dependence of $B_y(0)/B_1$ on the relative flow velocity is shown on Figure 4 for different values of the layer thickness, while keeping the value of $\theta_0 \approx 170°$. In Figure 4 the relative flow velocity $2U$ is normalized to $2V_{Ti}$, that is, $U/V_{Ti} = u\rho_i/(2D)$, while the thickness is measured in ion Larmor radius and expressed in terms of the parameter L of the Harris model by using the relation $L/\rho_i \approx 2D/\rho_i$ (see equation (11) for the case where the asymptotic fields are nearly antiparallel). It can be seen that decreasing/increasing the value of the relative flow velocity can lead to the same intensity of $B_y(0)/B_1$, provided the thickness is increased/decreased. On the other hand, the factor of asymmetry u [$=U/U_d = (U/V_{Ti})(2D/\rho_i)$] is directly proportional to D. Clearly, for a fixed value of U/V_{Ti} this factor increases proportionally to the thickness of the layer (L/ρ_i), because of a decrease of the ion drift velocity (U_d). This results in a decrease of s_0 (see Table 1) and, consequently, from pressure balance equation (22), to an increase of $B_y(x = 0)/B_1$, as illustrated in Figure 4. This increase of $B_y(0)/B_1$ with L, for a fixed U, can be explained by the new distribution of the current density, resulting from the larger value of the thickness, which modifies the integrated

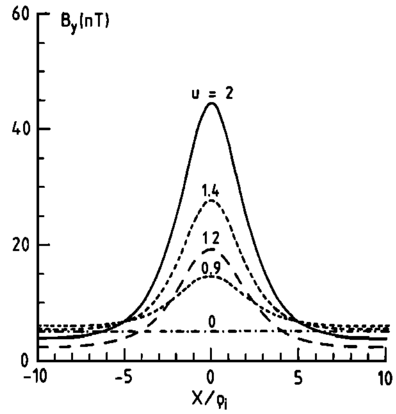

Fig. 3. Profiles of the B_y component of the magnetic field for different values of the flow asymmetry factor u. The value of s_0 (the number density of "trapped" particles at $x = 0$) depends on the value of u as indicated in Table 1. For all cases considered in this figure the total angle of rotation of the magnetic field through the magnetopause is $\theta_0 \approx 170°$. The other plasma and field parameters are the same as those used to compute Figures 1 and 2.

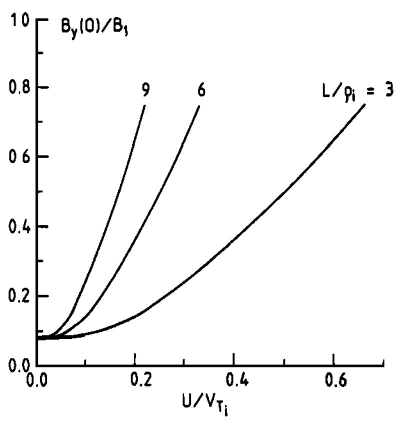

Fig. 4. Dependence of the B_y component of the magnetic field at $x = 0$ (normalized on B_1) on the shear flow U (normalized on V_{Ti}) for different values of the MCL thickness, while keeping the value of $\theta_0 \approx 170°$. In this figure the thickness is measured in the ion Larmor radius and is expressed in terms of the parameter L of the Harris model by using the relation $L/\rho_i \approx 2D/\rho_i$ (see equation (11) for the case where the asymptotic fields are nearly antiparallel). It can be seen that decreasing the value of the shear flow can lead to the same intensity of the B_y component at $x = 0$, provided the thickness is increased.

z component of the current density $\int_{-\infty}^{0} J_z\,dx$, responsible for the generation of $B_y(0)$. This integrated component, which is proportional to UL, is indeed increasing with the growth of L for a fixed U, while the integrated y component $\int_{-\infty}^{+\infty} J_y\,dx \sim U_d L$, supporting the initial (Harris) inversion of the magnetic field or the total variation of B_z ($\approx 2B_1$) is independent of L. Thus the thicker the Harris layer given by configuration (1) (with $B_y \ll B_0$), the easier "to spoil" it by smaller values of the relative flow velocity.

For $\theta_0 \to 180°$, when it is difficult to choose the shortest way of rotation [*Berchem and Russell*, 1982*b*], the sense of magnetic field rotation (determined by the sign of B_y) depends on the direction of the flow (the sign of U); that is, it may be opposite in the northern and southern hemispheres (there are some experimental data, discussed by *Sonnerup and Cahill* [1968] and *Su and Sonnerup* [1968], confirming this assumption).

4. Eigenmode Equation for the Tearing Mode in Magnetic Field Reversal With Relative Flow Velocity

Let us consider the stability of the central magnetic surface $x = 0$ of the plasma configuration modeled in the previous section with respect to the excitation of low-frequency tearing-type electromagnetic perturbations. Such perturbations can be described by a correction of the unperturbed vector potential which depends on both x and z coordinates and on the time t

$$A_y = A(x)\exp(-\imath\omega t + \imath kz) \qquad (23)$$

where ω ($\approx \imath\gamma$) is the complex frequency and $\mathbf{k}$ is the wave vector directed along the z axis. The first-order perturbation of the velocity distribution function (f_{1j}) is obtained by integrating the linearized Vlasov equation along the unperturbed particle trajectory.

$$f_{1j} = \frac{\partial f_{0j}}{\partial P_{jy}}\frac{1}{c}A_y - \imath\frac{e_j}{c}\left(\omega\frac{\partial f_{0j}}{H_j} + k\frac{\partial f_{0j}}{P_{jz}}\right)\int_{-\infty}^{t} v_y A_y\,d\tau \qquad (24)$$

An eigenmode equation is obtained by considering the linearized Maxwell equation

$$A_y'' - k^2 A_y = -\frac{4\pi}{c}\sum_{j=e,i} e_j \int v_y f_{1j}\,d\mathbf{v} \qquad (25)$$

Assuming that all particles are magnetized and that the ion Larmor radius is small, the standard procedure of evaluating the trajectory integral can be used (see, for example, *Wang et al.* [1992]), and equation (25) can be reduced to the following differential form

$$A(x)A_y'' + B(x)A_y' + C(x)A_y = 0 \qquad (26)$$

$$A(x) = 1 - A_i \qquad (27)$$

$$B(x) = B_i \qquad (28)$$

$$C(x) = -k^2 - V_0 + \sum_{j=e,i} V_j + C_i \qquad (29)$$

The term

$$V_0 A_y = \frac{4\pi}{c}\frac{\partial J_y}{\partial a_y}A_y \qquad (30)$$

is responsible for the adiabatic interaction of electromagnetic perturbations with particles. It depends on the global plasma distribution and characterizes the power of the free energy of the tearing mode, which determines whether the current filamentation resulting in the formation of magnetic islands is energetically favorable.

The flow asymmetry modifies the well-known potential well

$$V_0 = B_z''/B_z = -2L^{-2}\cosh^{-2}(x/L) \qquad (31)$$

corresponding to the symmetrical Harris case ($u = 0$), in the following way

$$V_0 = \frac{B_z''}{B_z} + \frac{B_y B_y'}{B_z B_1 L} \qquad (32)$$

We can expect that with the potential well described by equation (32) the stability properties of the MCL will be modified.

The term $V_j A_y$ corresponds to the singular current due to the nonadiabatic response of particles near $x = 0$

$$V_j = \frac{2\omega_{pj}^2}{c^2}\sum_{\nu=1}^{2}\eta_j^{(\nu)}\zeta_j^{(\nu)}W_{2j}^{(\nu)} \qquad (33)$$

where

$$\zeta_j^{(\nu)} = \frac{\omega_\nu}{k_\parallel V_{Tj}}, \quad \omega_\nu = \omega - \omega_E + (-1)^\nu u\frac{B_z^2}{B^2}kU_d \qquad (34)$$

$$\omega_E = kc\frac{EB_y}{B^2}, \quad k_\parallel = k\frac{B_z}{B}$$

$$\eta_j^{(\nu)} = \frac{1}{n(x)\omega_\nu}\left(\omega n_j^{(\nu)} - q_j t_j\frac{\partial n_j^{(\nu)}}{\partial \bar{a}_z}kU_d\right) \qquad (35)$$

$$W_{2j}^{(\nu)} = \frac{B_y^2}{B^2}\left\{Z_2(\zeta_j^{(\nu)}) + 2u\frac{B_z}{B}\frac{U_d}{V_{Tj}}Z_1(\zeta_j^{(\nu)}) + \left(u\frac{B_z}{B}\frac{U_d}{V_{Tj}}\right)^2 Z_0(\zeta_j^{(\nu)})\right\} \qquad (36)$$

$$Z_n(\zeta) = \frac{1}{\sqrt{\pi}}\int_{-\infty}^{\infty}\frac{t^n\exp(-t^2)\,dt}{t - \zeta - \imath\epsilon\,\mathrm{sign}\zeta}, \quad \epsilon \to 0$$

In these equations, E ($= -\partial\phi/\partial x$) is the equilibrium electric field, $\omega_{pj} = (4\pi ne^2/m_j)^{1/2}$ are plasma frequencies, and Z_0 is the plasma dispersion function.

The singular current, which is strongly peaked near the singular surface $x = 0$, is controlled by the local values of plasma density and magnetic field and could be significantly modified by flow asymmetry for $U_d < U \ll V_{Ti}$ even though the local velocity is very small around $x = 0$.

Coefficients A_i, B_i, and C_i come from the finite ion Larmor radius corrections (diamagnetic current perturbation)

$$A_i = \frac{V_{Ti}^2}{V_A^2}\sum_{\nu=1}^{2}\eta_i^{(\nu)}\zeta_i^{(\nu)}W_{0i}^{(\nu)} \qquad (37)$$

$$B_i = 2\frac{B}{B_1}\frac{V_{Ti}^2}{V_A^2}\sum_{\nu=1}^{2}\xi_i^{(\nu)}\zeta_i^{(\nu)}W_{0i}^{(\nu)} \quad (38)$$

$$C_i = \frac{2}{V_A^2}\sum_{\nu=1}^{2}\omega_\nu^2\eta_i^{(\nu)} \quad (39)$$

where $V_A = B/(4\pi m_i n)^{1/2}$ is the Alfven speed

$$W_{0j} = \frac{B_z^2}{B^2}Z_0(\zeta_j^{(\nu)}) - W_{2j} \quad (40)$$

$$\xi_i^{(\nu)} = \frac{1}{n(x)\omega_\nu}\left\{\omega\left(\frac{\partial n_i^{(\nu)}}{\partial \bar{a}_z}\frac{B_z}{B} - \frac{\partial n_i^{(\nu)}}{\partial \bar{a}_y}\frac{B_y}{B}\right) - kU_d\left(\frac{\partial^2 n_i^{(\nu)}}{\partial \bar{a}_z^2}\frac{B_z}{B} - \frac{\partial^2 n_i^{(\nu)}}{\partial \bar{a}_z \partial \bar{a}_y}\frac{B_y}{B}\right)\right\} \quad (41)$$

The differential approach used for evaluating these terms is only valid for $\rho_i\partial/\partial x \ll 1$, that is, outside the region $|x| < \rho_i$. Thus in the singular region these coefficients can be neglected.

5. Influence of Shear Flow on Growth of the Collisionless Tearing Mode in Center of the Magnetopause Current Layer ($x = 0$) With Large Angles of Magnetic Field Rotation ($\theta_0 \approx 170°$)

The stability analysis of the guide field tearing mode ($B_y \neq 0$, $B_y = \text{const} \ll B_0$) performed by *Wang and Ashour-Abdalla* [1992], where the modification of the B_y component profile by flow asymmetry was neglected, is only appropriate for very thin layers ($L \to \rho_i$). In this section we will evaluate the growth rate of tearing mode by solving the dispersion equation (26) for thicker layers ($L/\rho_i \sim 3\div 9$, i.e., $U_d \ll V_{Ti}$).

5.1. Analytical Estimates

Let us first make analytical estimates of the growth rate. Contributions from diamagnetic current perturbation (terms A_i, B_i, C_i) in the dispersion relation are of the order of $(U/V_A)^2$. For shear flow much less than the Alfven speed ($U \sim U_d \ll V_A$) the diamagnetic current perturbation (terms with A_i, B_i, C_i) can be neglected in comparison with current filamentation (term with V_0). The dispersion relation (26) in this approximation acquires the form

$$\Delta'(kL, u) = L\int_0^\infty V_e\, dx \quad (42)$$

The right-hand side of equation (42) is proportional to the perturbed electric field work upon the singular electron current and describes the irreversible increase of resonant electron energy. The value of this integral is controlled by the local values of the magnetic field and electron density in the region of the singular surface $x = 0$ and can be easily estimated from expressions (33)-(36). The growth rate $\gamma(u)$ takes the form

$$\gamma(u) = \Delta'(kL, u)kL\frac{\omega_i}{\beta_0\sqrt{\pi}}\frac{T_e + T_i}{T_i}\sqrt{\frac{m_e T_e}{m_i T_i}}\left(\frac{\rho_i}{L}\right)^3\frac{B_z'(0)L}{B_y(0)} \quad (43)$$

where ω_i ($= eB_1/m_i c$) is the ion Larmor frequency, $\beta_0 = 8\pi n(0)(T_i + T_e)/B_1^2$. For $u = 0$, $\beta_0 = B_0^2/B_1^2 \approx 1$.

The term $\Delta'(kL, u)$ is proportional to the power of the free energy source available from current filamentation. This term contains information about the global distribution of plasma and magnetic field in the layer. One can get the value of $\Delta'(kL, u)$ by solving the eigenmode equation in the "outer region"

$$A_y'' - k^2 A_y - V_0 A_y = 0 \quad (44)$$

and evaluating the jump of the logarithmic derivative

$$\frac{1}{L}\Delta'(kL, u) = \frac{A_y'(x \to +0)}{A_y(x \to +0)} - \frac{A_y'(x \to -0)}{A_y(x \to -0)} \quad (45)$$

For the Harris model without flow ($u = 0$) the expression for Δ' can be calculated for arbitrary magnetic surfaces within the layer and are expressed through the associated Legendre functions [see *Kuznetsova and Zelenyi*, 1985, p. 367]. For $x = 0$ this expression reduces to the well-known form

$$\Delta'(kL, u = 0) = \Delta'_0 = \frac{1 - (kL)^2}{kL} \quad (46)$$

The free energy of perturbations modified by the flow asymmetry factor is illustrated in Figure 5. It is seen that the curves "u=0" (symmetrical Harris case) and "u=2" are close to each other only in the narrow interval of wavelength: 0.5< kL <0.8. For longwave perturbations, kL < 0.5, the free energy is strongly modified. Specifically, for $0 \ll kL = m^*$,

$$\left[\Delta'(kL = m^*, u)\right]^{-1} = 0 \quad (47)$$

For $kL \to m^*$ the perturbed vector potential A_y and, consequently, the normal perturbation of the magnetic field tend to zero near the singular surface $x = 0$. The $x = 0$ singular surface itself remains unperturbed; meanwhile the peripheral magnetic surfaces experience the rippling-type distortions instead of reconnection. Thus with the increase of the wavelength, the quasi-symmetrical tearing mode transforms into the asymmetrical kink mode. For such perturbations (with $A_y(0) \sim 0$) the contribution from terms $A_i A''_y$ and

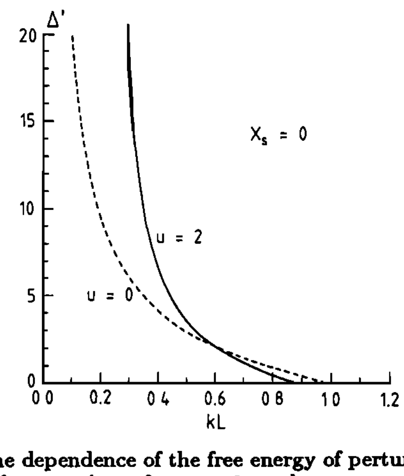

Fig. 5. The dependence of the free energy of perturbations Δ' of the central magnetic surface $x = 0$ on the wave number kL. The solid curve corresponds to a finite value of the flow asymmetry factor ($u = 2$). For comparison, the corresponding profile of Δ' for the symmetrical Harris configuration ($u = 0$) is illustrated by the dashed curve.

$B_i A'_y$ into the dispersion relation (26) could be essential. For $kL < m^*$ the free energy changes sign, and the mode of "negative energy" transforms therefore to the mode of "positive energy." Such transformation of the mode type in the longwave limit ($kL < m^* = x/L$) for perturbations of the peripheral magnetic surfaces ($x/L \neq 0$) in the symmetrical Harris configuration was considered in details in the paper by *Kuznetsova and Zelenyi* [1985].

Assuming that for shortwave ($m^* \ll kL < 0.8$) perturbations , $\Delta'(u) \approx \Delta'_0$, it is then easy to compare the growth rate of the tearing mode $\gamma(u)$, modified by the shear flow, with the well-known expression for the growth rate of the electron tearing mode (γ_e), excited in the center of the symmetrical Harris configuration

$$\frac{\gamma(u)}{\gamma_e} = \frac{n_0}{n(0)} \frac{B_{y0}}{B_y(0)} \frac{B'_z(0)L}{B_0} \quad (48)$$

where $n_0 = n(0)$ for $u = 0$, $B_{y0} = B_y(x \to \mp\infty) \ll B_z(x \to \mp\infty) = B_0$.

For $\theta_0 \approx 170°$ and $U > U_d$ the ratio $B_{y0}/B_y(0)$ could be very small. It is seen from equation (48) that the growth of the tearing instability will be significantly suppressed by the large value of the magnetic field $B_y(0)$ generated by the shear flow in the center of the current layer.

5.2. Numerical Results

The numerical solution of the dispersion equation (26) is performed by using the shooting method (see, for example, *Gladd* [1990] and *Wang and Ashour-Abdalla* [1992]). Coefficients $A(x)$, $B(x)$, and $C(x)$, which can be expressed through the initial profiles $a_y(x)$, $a_z(x)$, and $\phi(x)$, are calculated for the numerical equilibrium distribution obtained in section 3. As the values of $a_y(x)$, $a_z(x)$, and $\phi(x)$ are only known at some discrete points, the numerical integration of equation (26) must be coupled with a polynomial interpolation for determining those quantities at each step of integration.

Figure 6 shows the dependence of the maximum growth rate of the tearing instability on the factor of flow asymmetry u. It is seen that the growth rate decreases with increasing u. For $u \to 2$, corresponding to a relative flow $U = V_{Ti}\rho_i/D$ (which is much less than the ion thermal velocity V_{Ti}), the growth of the tearing mode significantly slows down.

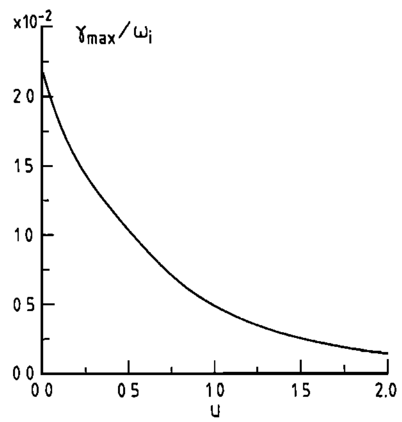

Fig. 6. The dependence of the maximum growth rate of the tearing instability (normalized on the ion Larmor frequency $\omega_i = eB_1/m_i c$) on the factor of flow asymmetry u.

6. Summary and Conclusions

The aim of this study is to understand some of the basic signatures of the internal structure of the magnetopause current layer separating plasmas with nearly opposite magnetic fields and with a relative flow velocity. The suggested simple kinetic self-consistent equilibrium model depends on parameters characterizing the flow asymmetry and determining the plasma density and magnetic field in the center of the layer. In the presence of a shear flow the magnetic field is expected to rotate from one direction to another, rather than to change its sign only. The structure of relatively thick layers ($L \sim 3 \div 9$) is significantly modified by comparatively small values of the shear flow (of the order of the ion drift speed). The modifications of the initial symmetrical Harris configuration (1), introduced by the presence of a shear flow, strongly influence the adiabatic interaction of the plasma with the tearing-type perturbations as well as the nonadiabatic response of the particles near the center of the MCL. In other words, the free energy of the perturbations (controlled by the global plasma and field distributions) and the singular current (controlled by the local values of the plasma density and magnetic field near the center of the MCL) are both significantly modified by the presence of a sheared flow. The growth rate of the collisionless electron tearing mode is decreased an order of magnitude when the relative flow velocity exceeds the ion drift velocity which for $L \sim 3 \div 9\rho_i$ is much smaller than the ion thermal speed. Thus the condition for reconnection beyond the stagnation region near the subsolar point, where the relative flow is small, is rather unfavorable.

It is reasonable to mention, concluding our discussion, that the results of the present study could also be applied to the magnetotail current layer, where a B_y component of the magnetic field is frequently observed [*Tsurutani et al.*, 1984; *Sergeev*, 1987]. The value of this component sometimes is rather large in comparison with the one that could penetrate inside the tail from the solar wind (V. A. Sergeev, private communication, 1991). Some asymmetry in the ion flow across the plasma sheet boundary layer, resulting in field-aligned currents, may become a source of generation of this dawn-dusk magnetic field, which is very important for magnetotail dynamics [*Büchner et al.*, 1991].

Acknowledgments. The authors would like to thank L. Zelenyi, P. Pritchett, B. Sonnerup, and J. Lemaire for fruitful discussions and valuable comments. Some of the computing work was performed at the San Diego Supercomputer Center. M.R. thanks the National Fund for Scientific Research (Belgium) for a research grant. M.M.K. and M.R. are also grateful to M. Ackerman, Director of the Belgian Institute for Space Aeronomy, for his support, which made the cooperation between both authors so enjoyable.

The editor thanks L-C. Lee and G. Ganguli for their assistance in evaluating this paper.

References

Alpers, W., Steady state charge neutral models of the magnetopause, *Astrophys. Space Sci.*, *5*, 425, 1969.

Berchem, J., and H. Okuda, A two-dimensional particle simulation of the magnetopause current layer, *J. Geophys. Res.*, *95*, 8133, 1990.

Berchem, J., and C. T. Russell, The thickness of the magnetopause current layer: ISEE 1 and 2 observations, *J. Geophys. Res.*, *87*, 2108, 1982a.

Berchem, J., and C. T. Russell, Magnetic field rotation through the magnetopause: ISEE 1 and 2 observations, *J. Geophys. Res.*, *87*, 8139, 1982*b*.

Bryant, D. A., and S. Riggs, At the edge of the Earth's magnetosphere: A survey by AMPTE-UKS, *Philoso. Trans. R. Soc. London, Ser. A*, *328*, 43, 1989.

Büchner, J., M. M. Kuznetsova, and L. M. Zelenyi, Sheared field tearing mode instability and creation of flux ropes in the Earth magnetotail, *Geophys. Res. Lett.*, *18*, 385, 1991.

Cai, D., L. R. O. Storey, and T. Neubert, Kinetic equilibria of plasma shear layers, *Phys. Fluids B*, *2*, 75, 1990.

Cargill, P. J., and T. E. Eastman, The structure of tangential discontinuities, 1, Results of hybrid simulations, *J. Geophys. Res.*, *96*, 13,763, 1991.

Coppi, B., J. W.-K. Mark, L. Sugiyama, and G. Bertin, Reconnecting modes in collisionless plasmas, *Phys. Rev. Lett.*, *42*, 1058, 1979.

Drake, J. F., and Y. C. Lee, Kinetic theory of tearing instabilities, *Phys. Fluids*, *20*, 1341, 1977.

Galeev, A. A., and L. M. Zelenyi, The model of magnetic field reconnection in a slab collisionless plasma sheath, *Pis'ma Zh. Eksp. Teor. Fiz.*, *25*, 407, 1977.

Galeev, A. A, M. M. Kuznetsova, and L. M. Zelenyi, Magnetopause stability threshold for patchy reconnection, *Space Sci. Rev.*, *44*, 1, 1986.

Ganguli, G., Y. C. Lee, and P. J. Palmadesso, Kinetic theory for electrostatic waves due to transverse velocity shears, *Phys. Fluids*, *31*, 823, 1988.

Gladd, N. T., Collisionless drift-tearing modes in the magnetopause, *J. Geophys. Res.*, *95*, 20,889, 1990.

Harris, E. G., On a plasma sheath separating regions of oppositely directed magnetic field, *Nuovo Cimento*, *23*, 115, 1962.

Hu, Y. D., Z. X. Lui, and Z. Y. Pu, Response of the magnetic field to the flow vortex field and reconnection in the magnetopause boundary region, *Sci. Sin. Ser. A Engl. Ed.*, *10*, 1100, 1988.

Kan, J. R., Equilibrium configurations of Vlasov plasmas carrying a current component along an external magnetic field, *J. Plasma Phys.*, *7*, 445, 1972.

Kuznetsova, M. M., and L. M. Zelenyi, Stability and structure of the perturbations of the magnetic surfaces in the magnetic transitional layers, *Plasma Phys. Controlled Fusion*, *27*, 363, 1985.

Kuznetsova, M. M., and L. M. Zelenyi, The theory of FTE: stochastic percolation model, in *Physics of Magnetic Flux Ropes, Geophys. Monogr. Ser.*, vol 58, edited by C. T. Russell, E. R. Priest, and L. C. Lee, p. 473, AGU, Washington, D.C., 1990*a*.

Kuznetsova, M. M., and L. M. Zelenyi, Nonlinear evolution of magnetic island in a sheared magnetic field with uniform plasma background, *Plasma Phys. Controlled Fusion*, *32*, 1183, 1990*b*.

La Belle-Hamer, A. L., Z. F. Fu., and L. C. Lee, A mechanism for patchy reconnection at the dayside magnetopause, *Geophys. Res. Lett.*, *15*, 152, 1988.

Lakhina, G. S., and K. Schindler, Collisionless tearing modes in the presence of shear flow, *Astrophys. Space Sci.*, *89*, 293, 1983*a*.

Lakhina, G. S., and K. Schindler, Tearing modes in the magnetopause current sheet, *Astrophys. Space Sci.*, *97*, 421, 1983*b*.

Lee, L. C., and J. R. Kan, A unified kinetic model of the tangential magnetopause structure, *J. Geophys. Res.*, *84*, 6417, 1979.

Lemaire, J., and L. F. Burlaga, Diamagnetic boundary layers: A kinetic theory, *Astrophys. Space Sci.*, *45*, 303, 1976.

Liu, Z. X., and Y. D. Hu, Local magnetic reconnection caused by vortices in the flow field, *Geophys. Res. Lett.*, *15*, 752, 1988.

Ofman, L., Double tearing instability with shear flow, *Phys. Fluids B*, *4*, 2751, 1992.

Press, W. H., B. P. Flannery, S. A. Teukolsky, and W. T. Vetterling, *Numerical Recipes: The Art of Scientific Computing*, Cambridge University Press, New York, 1986.

Pu, Z. Y., Kelvin-Helmholtz instability in collisionless space plasmas, *Phys. Fluids B*, *1*, 440, 1989.

Pu, Z. Y., and M. Yei, Coupling of the tearing mode instability with K-H instability at the magnetopause, in *Physics of Magnetic Flux Ropes, Geophys. Monogr. Ser.*, vol. 58, edited by C. T. Russell, E. R. Priest, and L. C. Lee, p. 493, AGU, Washington, D.C., 1990.

Pu, Z. Y., P. T. Hou, and Z. X. Liu, Vortex-induced tearing mode instability as a source of flux transfer events, *J. Geophys. Res.*, *95*, 18,861, 1990*a*.

Pu, Z. Y., M. Yei, and Z. X. Liu, Generation of vortex-induced tearing mode instability at the magnetopause, *J. Geophys. Res.*, *95*, 10,559, 1990*b*.

Quest, K. B., and F. V. Coroniti, Tearing at the dayside magnetopause, *J. Geophys. Res.*, *86*, 3289, 1981.

Ralston, A., and H. S. Wilf, *Méthodes Mathématiques Pour Calculateurs Arithmétiques*, Dunod, Paris, 1965.

Roth, M., Structure of tangential discontinuities at the magnetopause: The nose of the magnetopause, *J. Atmos. Terr. Phys.*, *40*, 323, 1978.

Roth, M., A microscopic description of interpenetrated plasma regions, in Magnetospheric Boundary Layers, edited by B. Battrick and J. Mort, *Eur. Space Agency Spec. Publ., ESA SP-148*, 295, 1979.

Roth, M., La structure interne de la magnétopause, *Mém. Cl. Sci. Acad. R. Belg. Collect. 8°*, *44*, 222 pp., 1984.

Sergeev, V. A., On the penetration of the B_y-component of the interplanetary magnetic field (IMF) into the tail of the magnetosphere (in Russian), *Geomagn. Aeron.*, *27*, 612, 1987. (*Geomagn. Aeron.*, Engl. Transl., *27*, 528, 1987.)

Sestero, A., Structure of plasma sheaths, *Phys. Fluids*, *7*, 44, 1964.

Sestero, A., Vlasov equation study of plasma motion across magnetic fields, *Phys. Fluids*, *9*, 2006, 1966.

Sonnerup, B. U. O., and L. J. Cahill, Jr., Explorer 12 observations of the magnetopause current layer, *J. Geophys. Res.*, *73*, 1757, 1968.

Su, S. Y., and B. U. O. Sonnerup, First-order orbit theory of the rotational discontinuity, *Phys. Fluids*, *11*, 851, 1968.

Tsurutani, B. T., D. E. Jones, R. P. Lepping, E. J. Smith, and D. G. Sibeck, The relationship between the IMF B_y and the distant tail (150–238 R_E) lobe and plasmasheet B_y fields, *Geophys. Res. Lett.*, *11*, 1082, 1984.

Wang, Z., and M. Ashour-Abdalla, Topological variation in the magnetic field line at the dayside magnetopause, *J. Geophys. Res.*, *97*, 8245, 1992.

Wang, Z., P. L. Pritchett, and M. Ashour-Abdalla, Kinetic effects on the velocity shear driven instability, *Phys. Fluids B*, *4*, 1092, 1992.

Whipple, E. C, J. R. Hill, and J. D. Nichols, Magnetopause structure and the question of particle accessibility, *J. Geophys. Res.*, *89*, 1508, 1984.

Zelenyi, L. M., and M. M. Kuznetsova, Large-scale instabilities of the plasma sheet driven by particle fluxes at the boundary of the magnetosphere, *Fiz. Plazmy Moscow*, *10*, 190, 1984.

M. Ashour-Abdalla and Z. Wang, Department of Physics and Institute of Geophysics and Planetary Physics, University of California, Los Angeles, CA 90024.

M.M. Kuznetsova, Space Research Institute, Russian Academy of Sciences, Profsoyuznaya 84/32, 117810 Moscow, Russia.

M. Roth, Institut d'Aéronomie Spatiale de Belgique, Avenue Circulaire 3, B-1180 Brussels, Belgium.

(Received January 20, 1993; revised July 2, 1993;
accepted August 13, 1993)